

# Identifying Unnecessary 3D Gaussians using Clustering for Fast Rendering of 3D Gaussian Splatting

Joongho Jo, Hyeongwon Kim, and Jongsun Park  
School of Electrical Engineering, Korea University, Seoul, Korea  
{jojoss1004, gusrnjs48, jongsun}@korea.ac.kr

## ABSTRACT

3D Gaussian splatting (3D-GS) is a new rendering approach that outperforms the neural radiance field (NeRF) in terms of both speed and image quality. 3D-GS represents 3D scenes by utilizing millions of 3D Gaussians and projects these Gaussians onto the 2D image plane for rendering. However, during the rendering process, a substantial number of unnecessary 3D Gaussians exist for the current view direction, resulting in significant computation costs associated with their identification. In this paper, we propose a computational reduction technique that quickly identifies unnecessary 3D Gaussians in real-time for rendering the current view without compromising image quality. This is accomplished through the offline clustering of 3D Gaussians that are close in distance, followed by the projection of these clusters onto a 2D image plane during runtime. Additionally, we analyze the bottleneck associated with the proposed technique when executed on GPUs and propose an efficient hardware architecture that seamlessly supports the proposed scheme. For the Mip-NeRF360 dataset, the proposed technique excludes 63% of 3D Gaussians on average before the 2D image projection, which reduces the overall rendering computation by almost 38.3% without sacrificing peak-signal-to-noise-ratio (PSNR). The proposed accelerator also achieves a speedup of  $10.7\times$  compared to a GPU.

## KEYWORDS

3D Gaussian splatting, Rendering, NeRF, Neural Radiance Field, Hardware Accelerator

## 1 INTRODUCTION

In 3D computer vision applications, such as augmented reality (AR), virtual reality (VR), and the metaverse, fast and high-quality image rendering is important. While rendering techniques using

deep neural networks such as neural radiance field (NeRF) [1], [2], [3] have been extensively studied, 3D Gaussian splatting (3D-GS) [4], a new rendering approach, has recently captured notable attention due to its ability to rapidly render high-quality images compared to conventional NeRF.

3D-GS represents complex 3D scenes by utilizing millions of 3D Gaussians and renders 3D scenes by projecting 3D Gaussians onto a 2D image plane. The rendering process consists of 2 main steps: 1) All 3D Gaussians are projected onto a 2D image plane, and the 3D Gaussians that influence the colors of a 2D image are identified. 2) The color of each pixel in the 2D image is then calculated using the identified 3D Gaussians that influence the color. In step 1 of the rendering process above, after a Gaussian is projected onto a 2D image but is identified as not influencing the 2D image’s color, the projection becomes a waste of computations. In the case of the Mip-NeRF360 dataset, on average, about 67.6% of 3D Gaussians do not influence the color of 2D images. So, these Gaussians can be excluded from the current view rendering process. However, since 3D Gaussians that influence the 2D image’s color can change depending on the position and direction of the rendering viewpoint, it remains challenging to identify unnecessary 3D Gaussians before their projection onto the 2D image plane. Consequently, these unnecessary 3D Gaussians still undergo projection calculations. Thus, if a simple yet efficient method could be developed to predict the 3D Gaussians that do not affect the 2D image’s color and exclude them before the rendering process starts, it could significantly reduce the overall computational complexity of the entire 3D-GS process.

In this paper, we propose a clustering-based approach to exclude unnecessary 3D Gaussians in the current view rendering process by identifying clusters that do not affect the 2D image’s color. The goal of clustering is to group closely located 3D Gaussians together, and the shape of the clusters should be spherical for easy projection onto a 2D image. Hence, we employ the K-means clustering algorithm, which meets these two criteria. Given that 3D Gaussians possess a size or influence defined by their covariance, the radii of the cluster spheres are determined not only by the distance to the cluster’s centroid but also by considering the size of the Gaussians. These defined cluster spheres are then projected onto a 2D image plane to determine their influence on the 2D image’s color. Clusters that do not affect the image color can be excluded from the rendering process. In our approach, clustering and calculating the radii of clusters can be executed offline, and only projecting clusters onto the 2D image plane is performed in real time, which takes only 6.2% of computation overhead. In the 3D-GS rendering process, when applying the proposed approach before the current

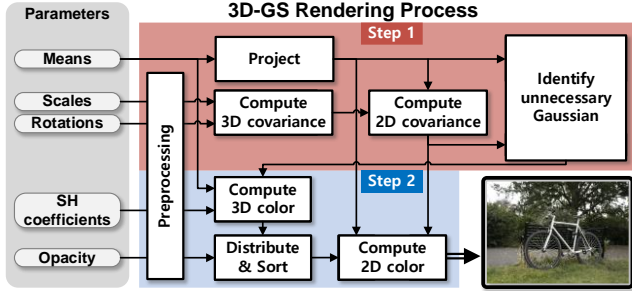


Fig. 1: The overall rendering process of 3D Gaussian Splatting (3D-GS) [4] and the input parameters.

view rendering process starts, we can exclude (pre-screen) approximately 63.1% of 3D Gaussians in the Mip-NeRF360 dataset. For the excluded 3D Gaussians, the following step 1 operation of the rendering process can be omitted, leading to significant computational complexity reduction in the 3D-GS process. When applying the proposed clustering-based approach to 3D-GS rendering on a GPU, a significant amount of time is taken in the process of packing data, leading to only marginal improvements in speed. Therefore, in this work, we also introduce a hardware architecture that supports the proposed technique by employing ping-pong buffers and cluster ordering.

Our contributions are summarized as follows:

- To the best of our knowledge, this is the first work to propose a technique for pre-identifying unnecessary 3D Gaussians based on the current view direction before starting 3D-GS rendering.
- We introduce a method to determine cluster sizes, considering the influence of 3D Gaussians, and a method for projecting clusters onto a 2D image.
- Extensive experiments demonstrate the efficiency of our technique in identifying unnecessary 3D Gaussians without compromising the peak signal-to-noise ratio (PSNR).
- A hardware architecture is proposed to facilitate the seamless execution of the proposed technique.

## 2 BACKGROUND AND MOTIVATION

### 2.1 Parameters and Overall Rendering Process of 3D Gaussian Splatting

Fig. 1 illustrates the overall rendering process of 3D-GS [4] and the input parameters of 3D Gaussians. A 3D Gaussian is composed of 5 parameters (means, scales, rotations, spherical harmonics (SH) coefficients, opacity), all of which are the values trained through backpropagation operations. The three means of the 3D Gaussian represent the center coordinates ( $x$ ,  $y$ ,  $z$ ) of the 3D Gaussian in world coordinates. Scales and rotations correspond to the elements of the scale matrix and rotation matrix, which are used to calculate the covariance matrix of the 3D Gaussian during the rendering process [4]. SH coefficients [5], [6] are used to calculate the color of the 3D Gaussian, and opacity is used in the color computations of the 2D image to be rendered.

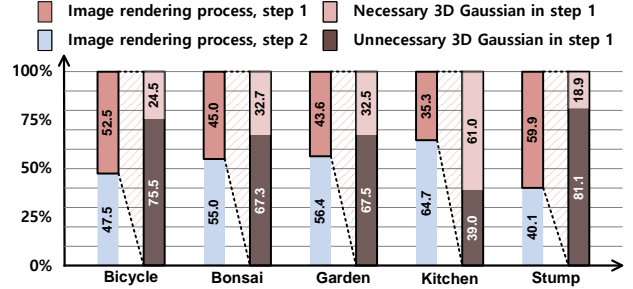


Fig. 2: Normalized latency breakdown and the proportion of unnecessary 3D Gaussians in step 1

As shown in Fig. 1, the rendering process of 3D-GS is primarily divided into 2 steps. In the first step, the center coordinates (means) of the 3D Gaussian are initially transformed from a world coordinate system to a camera coordinate system. Then, the transformed coordinates are projected to the 2D image plane. (world, camera, and image coordinate systems are visualized in Fig. 3). Using scales and rotations, 3D and 2D covariances are calculated [7], and the size of the Gaussian in the 2D image is determined based on the 3 sigma (standard deviation) rule [6]. Finally, by using the size and coordinates in the image coordinate system, 3D Gaussians that influence the color of the 2D image of the current view rendering are identified. The second step is illustrated in the lower area in Fig. 1. The parameters of 3D Gaussian that are identified as influencing the 2D image’s color are only utilized. The SH coefficients, opacity, and the coordinates calculated in step 1 are employed to calculate the 2D color. Although not illustrated in the figure, camera intrinsic/extrinsic parameters for the current view are used in both steps.

### 2.2 Motivation

Key observations in the conventional 3D-GS rendering process include 1) the presence of many unnecessary 3D Gaussians in the current view rendering, and 2) the fact that step 1 operations are performed on all 3D Gaussians to identify unnecessary ones. Fig. 2 illustrates the GPU (RTX A6000) runtime breakdown and the proportion of unnecessary 3D Gaussians for the 3D-GS-30k pre-trained model, using the Bicycle, Bonsai, Garden, Kitchen, and Stump scenes of the Mip-NeRF360 dataset [3]. As shown in the figure, step 1 accounts for approximately 51.3% of the total latency, and as a result of step 1, about 65.7% of all 3D Gaussians are identified as unnecessary. In other words, about 65.7% of the 3D Gaussians are ones that did not need to undergo step 1 operations. Consequently, it is anticipated that significant computational reductions can be achieved if unnecessary 3D Gaussians can be identified before step 1.

### 2.3 Analysis of Unnecessary 3D Gaussians

Fig. 3 illustrates the necessary and unnecessary regions of an example image in the rendering process. In the figure, three coordinate systems are depicted: black arrows represent the world coordinate system, blue ones denote the camera coordinate system, and red signifies the image coordinate system. As observed in the

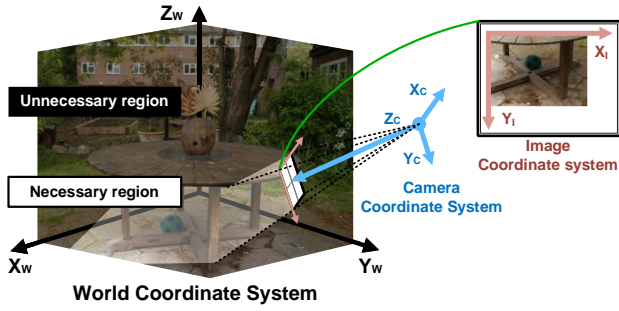


Fig. 3: Illustrating the necessary and unnecessary region of the rendering process.

figure, when the viewpoint and direction are determined, the necessary region for the image rendering is identified (illustrated in the bright). The region that is either opposite to the image direction or does not enter the image boundary is considered unnecessary for the current view rendering (illustrated in the dark). Since 3D-GS represents 3D scenes by utilizing millions of 3D Gaussians, 3D Gaussians representing *unnecessary region* is considered unnecessary 3D Gaussians for the current view rendering. In other words, *it can be observed that the unnecessary 3D Gaussians are closely located to each other in the world coordinate system*. This observation motivated our exploration of distance-based clustering as a potential solution to the computational waste issue.

In section 3, we present a simple clustering-based technique to identify unnecessary 3D Gaussians for the current view rendering before the 2D image projection without compromising image quality.

### 3 CLUSTERING BASED IDENTIFYING TECHNIQUE

#### 3.1 Overall Rendering Process with the Proposed Technique

Fig. 4 visually represents the overall process of the proposed technique as follows: **Offline**) Cluster the 3D Gaussians, and calculate the radius of each cluster. **Step 0**) During real-time rendering, project the clusters onto the 2D image plane based on the current view direction. Utilize the projected clusters to identify which clusters influence the 2D image colors. **Steps 1 and 2**) Proceed with the conventional rendering process only for 3D Gaussians identified in step 0.

In the proposed approach, the K-means clustering algorithm is employed, and the cluster radius is decided considering the size of the 3D Gaussians. Detailed explanations are described in sections 3.2 and 3.3.

#### 3.2 Clustering Method

The proposed technique employs the K-means clustering algorithm [10], which assumes spherical-shaped clusters and is distance-based. The reason for defining the shape of the cluster as spherical is to facilitate easy projection onto the 2D image plane, as considering only the center and radius of the sphere make its

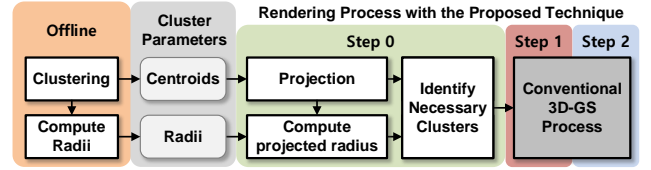


Fig. 4: The overall rendering process with the proposed technique.

projection straightforward onto the 2D image plane. If the shape of the cluster is not spherical but some other shape, the shape of the cluster projected onto the 2D image plane would continuously change depending on the viewpoint, making it difficult to calculate the cluster's influence. The reason for selecting distance-based clustering is that the purpose of clustering is not to classify data or detect outliers, but to group 3D Gaussians that are close in distance to determine at once whether they are unnecessary for the current view rendering.

#### 3.3 Radii of Cluster Spheres

A 3D Gaussian is not a single point but a distribution. So, simply defining the radius of a cluster as the distance between the center of the cluster and the center of the Gaussian might not accurately reflect the influence of the 3D Gaussian. Hence, we define the size of the 3D Gaussian based on the statistics and subsequently define the cluster radius considering the size of the Gaussian. In the statistics, the standard deviation (sigma) of the longest direction of a 3D Gaussian is defined as the largest value among the square roots of the eigenvalues of the 3D covariance matrix ( $3 \times 3$ ). So, we use the eigenvalues of the 3D covariance and the 3-sigma rule to define the size of the 3D Gaussian. The 3-sigma rule is a method that utilizes the principle that 99.7% of the data lies within 3 standard deviations. The equation of the size of the 3D Gaussian is as follows:

$$SG_i = 3 \times \sqrt{\max(\lambda_{1,i}, \lambda_{2,i}, \lambda_{3,i})}. \quad (1)$$

In (1),  $SG_i$  is  $i$ -th size of the 3D Gaussian,  $\lambda$  means the eigenvalues of the 3D covariance matrix. The radius of the cluster sphere can be expressed as follows:

$$RC_j = \max_{i \in j} (\text{dist}(\text{centroid}_j, \text{gaussian}_i) + SG_i). \quad (2)$$

In (2),  $RC_j$  represents the radius of the  $j$ -th cluster, and  $\text{dist}(\text{centroid}_j, \text{gaussian}_i)$  refers to the distance between the center of the  $j$ -th cluster and the center of the  $i$ -th Gaussian belonging to that cluster. Thus, (2) defines the cluster radius as the maximum value among the distances between the cluster center and the Gaussian center plus the size of the Gaussian defined in (1).

#### 3.4 Radius of Projected Cluster

As explained in section 3.1, in the proposed technique, clusters are projected onto a 2D image plane to identify unnecessary 3D Gaussians. So, we need to know the radius of the circle (2D image plane) on which the defined cluster sphere is projected. Fig. 5

TABLE I. SIMULATION RESULTS

Dataset	Tanks&Temples						Deep Blending					
	Train			Truck			Playroom			Dr. Johnson		
Metric	PSNR	SSIM	Exclusion rate	PSNR	SSIM	Exclusion rate	PSNR	SSIM	Exclusion rate	PSNR	SSIM	Exclusion rate
Baseline	21.77	0.8045	36.64%	24.94	0.8710	65.46%	29.93	0.9006	86.96%	28.94	0.8963	86.46%
Ours (only distance)	21.45	0.8025	<b>33.97%</b>	24.72	0.8701	<b>64.11%</b>	29.91	0.9002	<b>86.75%</b>	28.90	0.8953	<b>86.31%</b>
Ours (dist. + radius)	<b>21.77</b>	<b>0.8045</b>	28.01%	<b>24.94</b>	<b>0.8710</b>	60.45%	<b>29.93</b>	<b>0.9006</b>	83.57%	<b>28.94</b>	<b>0.8963</b>	83.58%

Dataset	Mip-NeRF360											
	Bicycle			Bonsai			Counter			Garden		
Metric	PSNR	SSIM	Exclusion rate									
Baseline	25.17	0.7625	75.50%	31.98	0.9377	67.32%	28.89	0.9048	56.44%	27.18	0.8607	67.46%
Ours (only distance)	25.10	0.7620	<b>74.92%</b>	31.91	0.9375	<b>66.43%</b>	28.76	0.9038	<b>54.83%</b>	27.10	0.8604	<b>67.07%</b>
Ours (dist. + radius)	<b>25.17</b>	<b>0.7625</b>	73.76%	<b>31.98</b>	<b>0.9377</b>	63.52%	<b>28.89</b>	<b>0.9048</b>	49.42%	<b>27.18</b>	<b>0.8607</b>	64.31%

Dataset	Kitchen			Room			Stump			Treehill		
	Metric	PSNR	SSIM	Exclusion rate	PSNR	SSIM	Exclusion rate	PSNR	SSIM	Exclusion rate	PSNR	SSIM
Baseline	30.71	0.9227	39.05%	31.34	0.9158	76.28%	26.56	0.7702	81.09%	22.30	0.6307	77.58%
Ours (only distance)	30.51	0.9222	<b>36.87%</b>	30.70	0.9147	<b>75.51%</b>	26.54	0.7699	79.94%	22.27	0.6303	<b>76.88%</b>
Ours (dist. + radius)	<b>30.71</b>	<b>0.9227</b>	31.71%	<b>31.34</b>	<b>0.9158</b>	69.95%	<b>26.56</b>	<b>0.7702</b>	77.25%	<b>22.30</b>	<b>0.6307</b>	74.50%

illustrates the projection of a sphere. In the figure,  $W$  is the width of the rendered image, and  $\theta$  is the camera's field of view (FOV); these two values are given as input once the viewpoint is determined. In the figure,  $R$  is the radius of the cluster sphere, calculated as (2), and  $D$  is the perpendicular distance between the viewpoint and the cluster sphere, which is the z-value when the cluster center is transformed into the camera coordinate system.  $r$  is the radius of the projected circle, and  $d$  is the perpendicular distance between the viewpoint and the 2D image plane, calculated as

$d = W / (2 \times \tan(\theta/2))$ . Furthermore, using the formula of similar triangles,  $r:R = d:D$ ,  $r$  is expressed by the following equation:

$$r = \frac{R \times W}{2 \times \tan(\theta/2) \times D}. \quad (3)$$

Through (3), the radius of the projected cluster is quickly calculated during real-time rendering.

### 3.5 Simulation Results

**Simulation environment setting:** We evaluate the performance of the proposed technique on the two scenes from the Tanks&Temples dataset [8], the two scenes from the Deep Blending [9], and eight sets of scenes presented in Mip-NeRF360 [3]. 3D-GS-30k pre-trained model [4] on an RTX A6000 GPU is used for the simulation. A train/test split for the datasets is employed, following the methodology proposed by Mip-NeRF360, where every 8th photo is used for testing. To generate error metrics, we use the standard peak signal-to-noise ratio (PSNR) and structural similarity index measure (SSIM) metrics.

Table I presents the simulation results. In the table, 'baseline' represents the results of the conventional 3D-GS method. 'Exclusion rate' in the baseline refers to the percentage of 3D Gaussians excluded from calculation after step 1, representing the ideal 3D Gaussians excluded ratio. On the other hand, the 'Exclusion rate' in 'ours' indicates the percentage of 3D Gaussians pre-excluded from calculation before the rendering process using the proposed technique. As shown in the table, when the radius of

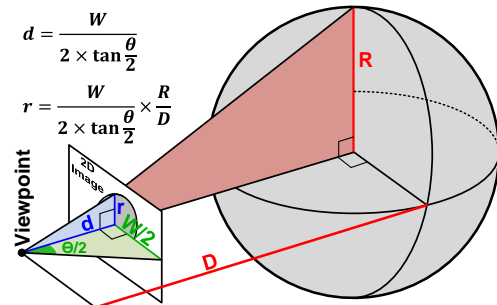


Fig. 5: Visualizing the mathematical representation of sphere projection onto a 2D image plane.

a cluster is calculated solely based on the distance between the Gaussian center and the cluster center (Ours (only distance)), the smaller radius results in more 3D Gaussians being excluded. However, since the influence of the cluster is not adequately reflected in the radius calculation, the PSNR decreases. In contrast, when the cluster radius is calculated considering the influence of the 3D Gaussians (Ours (dist. + radius)), although the proportion of excluded 3D Gaussians decreases, there is no reduction in PSNR and SSIM compared to the baseline.

To summarize, the proposed technique enables the average exclusion (pre-screening) of 44.23%/83.56%/63.05% of 3D Gaussians before starting the current view rendering in Tanks&Temples/Deep Blending/Mip-NeRF360 datasets, without any degradation in image quality. The simulation results demonstrate that using the clustering technique alone can achieve a high exclusion rate with a slight decrease in PSNR, while calculating the cluster radius considering the influence of 3D Gaussians can achieve an exclusion rate close to the baseline without sacrificing PSNR, and SSIM.

## 4 HARDWARE ARCHITECTURE

### 4.1 Motivation

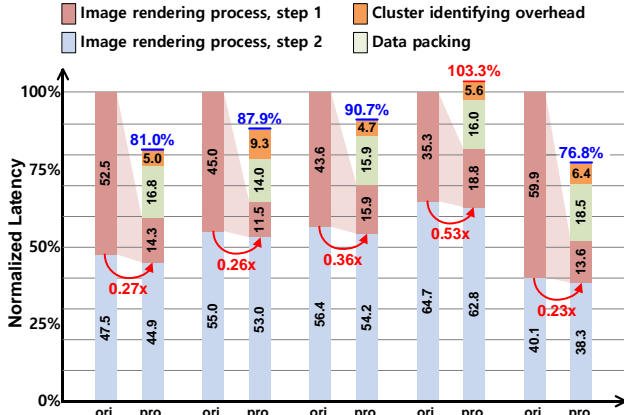


Fig. 6: Runtime breakdown of the conventional 3D-GS rendering process and the rendering process with the proposed technique.

Fig. 6 shows a runtime breakdown of 3D-GS rendering with the proposed technique applied to various 3D scenes when running on a GPU. In the figure, ‘ori.’ represents the conventional 3D-GS rendering process, and ‘pro.’ denotes the rendering process with the proposed technique applied. The experiment is conducted on an RTX A6000 GPU. As illustrated in the figure, the latency for the step 1 operation has been reduced by an average of 66.9%. But, despite the reduction in step 1 computation, the expected speed improvement is not achieved for two main reasons. First, due to the SIMD parallel processing characteristics of the GPU, step 1 cannot be started until the cluster identification operation is complete. If the step 1 operation could be started immediately after the some of cluster identification is complete, the overhead of the identification process could be hidden during execution time. Second, in order to start the step 1 operation, the identified data is first extracted and packed from the existing data. This is due to the characteristic of the GPU that it processes data in parallel at once. In the case of the Kitchen scene, it is observed that the number of excluded 3D Gaussians is small, leading to more overhead than the reduction in step 1 latency. Therefore, in section 4.2, we propose a hardware architecture that efficiently implements the proposed technique through ping-pong buffers and cluster ordering.

## 4.2 Architecture Overview and Timing Diagram

Fig. 7 shows the overall architecture of the proposed accelerator. The proposed accelerator consists of three primary components: **Cluster Identification Engine (CIE)**: Responsible for identifying clusters relevant to the current view and those that can be excluded. It utilizes a first in first out (FIFO) buffer for cluster centroid and radius storage, a 4x4 processing elements (PE) array for projection matrix multiplication, and a 2D Radii Calculator module for (3) calculations. All CIE operations are performed independently for each cluster, enabling parallel processing. **Step 1 Engine**: Handles the first stage of the conventional rendering tasks. It employs a local ping-pong buffer to store means, scales, and rotations of 3D Gaussians identified as necessary for rendering by the CIE. Once a ping-pong buffer fills, step 1 operations commence, including

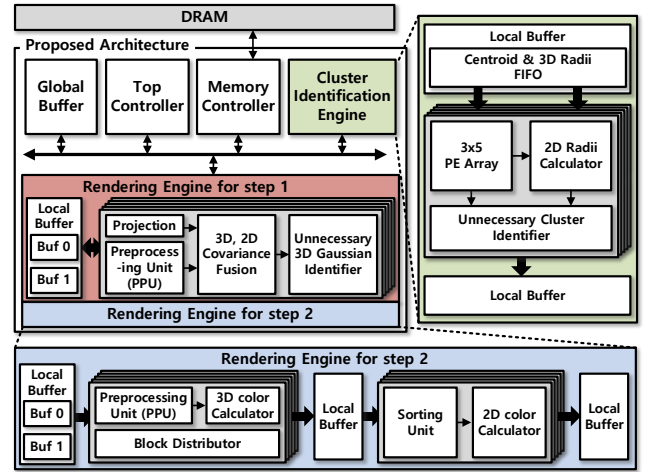


Fig. 7: Overall architecture of the proposed accelerator, illustrating the block diagram of three main components 1) Clustering Identification Engine, 2) Step 1 Engine and 3) Step 2 Engine.

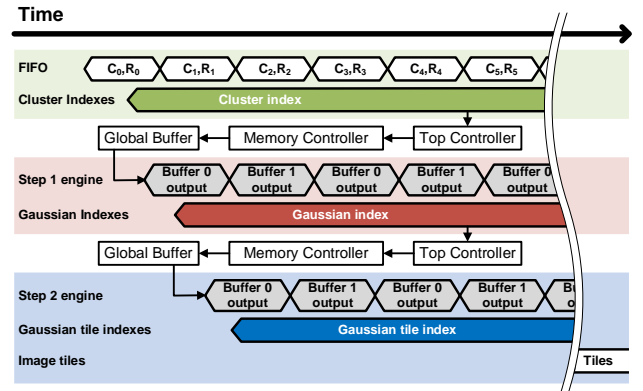


Fig. 8: Computation pipeline diagram of the proposed architecture.

projection computation, preprocessing, covariance calculation, and unnecessary Gaussian identification. All Step 1 operations are performed independently (in parallel) for each 3D Gaussian. **Step 2 Engine**: Responsible for the second stage of conventional rendering tasks. It also utilizes a local ping-pong buffer to store the results of step 1, including SH coefficients, and the opacity values of 3D Gaussians identified by Step 1. Upon filling a buffer, step 2 operations begin. Unlike step 1 engine, step 2 incorporates a Gaussian distribution module that distributes Gaussians affecting color calculation to different image tiles. After distribution, Gaussians within each tile are sorted based on their proximity to the 2D image, followed by 2D color computation. Preprocessing, 3D color computation, and the Gaussian distribution module enable parallel processing at the Gaussian level, while sorting and subsequent steps facilitate parallel processing at the tile level.

Fig. 8 illustrates the timing diagram of the proposed hardware: 1) The centroid (C) and radius (R) values of the clusters are loaded into the FIFO queue of the ‘Cluster Identification Engine’, and each cluster is processed in parallel. 2) The 3D Gaussian data belonging

TABLE II. A SUMMARY OF THE DEVICES' SPECIFICATIONS.

	Ours	Nvidia RTX A6000
Area	9.94mm <sup>2</sup>	628mm <sup>2</sup>
Frequency	500MHz	1410MHz
DRAM Bandwidth	25.6GB/s	768GB/s
SRAM	1MB	6MB
Technology	28nm	8nm
Power	3.5W	300W

to the identified cluster are loaded from the global buffer into one of the ping-pong buffers of the step 1 engine. 3) When the ping-pong buffer is full, the step 1 operations start. 4) The Gaussian data identified by step 1 are loaded from the global buffer into one of the ping-pong buffers of the step 2 engine. 5) When the ping-pong buffer is full, the step 2 operation begins. As presented in the timing diagram, ping-pong buffer scheduling and its utilization allow for the seamless implementation of the proposed technique in hardware.

### 4.3 Cluster Ordering

The number of clusters in a 3D scene can vary from thousands to tens of thousands. This makes it challenging to simultaneously identify unnecessary clusters in parallel for all the clusters. As a result, the main rendering operations (the step 1 engine and the step 2 engine) can remain idle until necessary clusters for the current view rendering are identified in CIE. Consequently, one of the challenges is determining the order of cluster operations to minimize this waiting time. Based on this analysis, we prioritize clusters with a high probability of selection to minimize the waiting time of the step 1 engine and step 2 engine. Then, the global buffer also retrieves data from DRAM according to priority.

### 4.4 Hardware Results

The dedicated accelerator supporting the proposed technique has been implemented using a 28nm CMOS process. The architecture was first coded in Verilog and synthesized with Synopsys Design Compiler. Power and energy consumption were simulated using Synopsys PrimeTime-PX. The speedup was obtained using an in-house developed cycle-accurate simulator, with a DRAM bandwidth of 25.6GB/s, and the DRAM energy is computed based on [11]. and Table II presents the comparisons between the proposed accelerator and the baseline.

Fig. 9 illustrates a graph comparing the rendering speeds of the conventional 3D-GS and the proposed technique on the RTX A6000, with the same comparison conducted on the proposed architecture. The dataset used is MiP-NeRF360. When the proposed technique is implemented on the GPU, an average speed improvement of 1.12x is observed compared to the conventional 3D-GS. Applying the proposed clustering-based technique on the proposed hardware results in an average speed increase of 1.31x compared to the conventional 3D-GS. This demonstrates that the proposed technique effectively reduces the computational load compared to the GPU. When comparing the GPU with the proposed hardware, there is a maximum speed improvement of 13.3x and an average improvement of 10.7x.

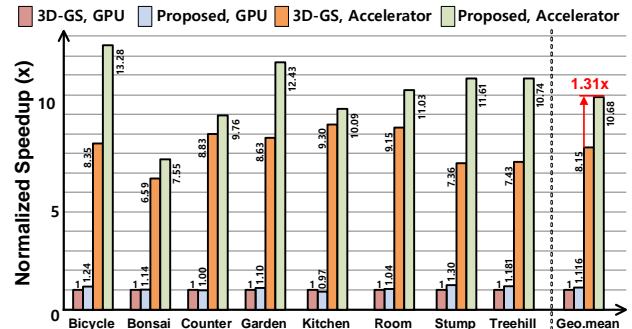


Fig. 9: The normalized speedup achieved by our proposed architecture and RTX A6000 on the eight scenes of MiP-NeRF360.

## 5 CONCLUSION

We introduce a clustering-based technique for the 3D-GS rendering process to substantially reduce computational burden by pre-identifying unnecessary 3D Gaussians without sacrificing image quality. To enhance the accuracy of pre-identification, we propose a method for defining the radius of clusters by considering the influence of the 3D Gaussians and projecting the clusters onto a 2D image. In a hardware implementation, a ping-pong buffer is employed to improve speed and energy-efficiency, prioritizing clusters with high usage frequencies. We believe that this work presents a novel and cost-effective perspective on the efficient processing of 3D-GS rendering.

## REFERENCES

- MILDENHALL, Ben, Pratul P. Srinivasan, et al. "NeRF." Communications of The ACM, December 17, 2021. <https://doi.org/10.1145/3503250>.
- MÜLLER, Thomas, Alex Evans, et al. "Instant Neural Graphics Primitives with a Multiresolution Hash Encoding." ACM Transactions on Graphics, July 1, 2022. <https://doi.org/10.1145/3528223.3530127>.
- BARRON, Jonathan T., et al. Mip-nerf 360. In: Proceedings of the IEEE/CVF Conference on Computer Vision and Pattern Recognition. 2022. p. 5470-5479.
- KERBL, Bernhard, Georgios Kopanas, et al. 3D gaussian splatting for real-time radiance field rendering. ACM Transactions on Graphics (ToG), 2023, 42.4: 1-14.
- FRIDOVICH-KEIL, Sara, Alex Yu, et al. Plenoxels: Radiance fields without neural networks. In: Proceedings of the IEEE/CVF Conference on Computer Vision and Pattern Recognition. 2022. p. 5501-5510.
- PUKELSHEIM, Friedrich. "The Three Sigma Rule." The American Statistician 48, no. 2 (1994): 88-91. <https://doi.org/10.2307/2684253>.
- ZWICKER, Matthias, Hanspeter Pfister, et al. EWA volume splatting. In: Proceedings Visualization, 2001. VIS'01. IEEE, 2001. p. 29-538.
- KNAPITSCH, Arno, Jaesik Park, et al. Tanks and temples: Benchmarking large-scale scene reconstruction. ACM Transactions on Graphics (ToG), 2017, 36.4: 1-13.
- HEDMAN, Peter, Julien Philip, et al. Deep blending for free-viewpoint image-based rendering. ACM Transactions on Graphics (ToG), 2018, 37.6: 1-15.
- LLOYD, Stuart. Least squares quantization in PCM. IEEE transactions on information theory, 1982, 28.2: 129-137.
- Z. Zhou, J. Liu, Z. Gu and G. Sun, "Energon: Toward Efficient Acceleration of Transformers Using Dynamic Sparse Attention," in IEEE Transactions on Computer-Aided Design of Integrated Circuits and Systems, vol. 42, no. 1, pp. 136-149, Jan. 2023, doi: 10.1109/TCAD.2022.3170848.